

A generalized multiple dependent state sampling chart based on ridge penalized likelihood ratio for high-dimensional covariance matrix monitoring

Maziar Saemian¹, Ali Salmasnia^{*2}, and Mohammad Reza Maleki³

¹*Department of Industrial Engineering, University of Eyvanekey, Semnan, Iran*

²*Department of Industrial Engineering, Faculty of Engineering, University of Qom, Iran*

³*Industrial Engineering Group, Golpayegan College of Engineering, Isfahan University of Technology, Golpayegan, 87717-67498, Iran*

Abstract

Online monitoring of high-dimensional processes variability in which the number of variables is larger than the sample size is a challenging issue for quality practitioners because the sample covariance matrix is not invariable. To deal with this challenge, a generalized multiple dependent state sampling (*GMDS*) chart based on ridge penalized likelihood ratio (*RPLR*) statistic is developed for Phase II monitoring of multivariate process variability under high-dimensional setting. The developed control chart benefits from three advantages: (1) departing from the conventional covariance matrix charts, it can be efficiently employed for both spars and non-spars covariance matrices; (2) it is able to detect spars shift patterns in which only a few covariance matrix elements are deviated from their nominal values; and (3) it outperforms the detectability of the *RPLR* chart in terms of average run length (*ARL*) and standard deviation of run length (*SDRL*). The performance of *RPLR*, *MDS-RPLR*, and *GMDS-RPLR* charts are compared using extensive simulation studies by considering different diagonal and/or off-diagonal covariance matrix disturbances. Moreover, sensitivity analysis are provided to analyze how the number of process variables and *GMDS* parameter affect the run length properties of the developed chart.

Keywords: Covariance matrix, High-dimensionality, Ridge penalized likelihood ratio, Generalized multiple dependent state sampling, Spars disturbances.

1. Introduction

Control charts can be categorized into univariate and multivariate charts based on the number of underlying quality characteristics. Considering the correlation structure among quality

* Corresponding author: a.salmasnia@qom.ac.ir, +989122865720

characteristics, multivariate control charts are efficient tools to detect sustained shifts in process parameters when the sample size is larger than the number of study quality characteristics. However, today's competitive business has forced companies to address a significant number of quality dimensions for fulfilling their customers' expectations, increasing market share as well as keeping competitive advantages. Hence, it is essential for quality engineering researches to dedicate their attempts to settle a vast amount of recorded data in which the process dimension exceeds the sample size. In this regard, control charts available in statistical process monitoring (SPM) literature are not usually efficient to analyze many pieces of information. To overcome the curse of high-dimensionality, some monitoring schemes such as variable selection-based multivariate charts, set-wise exponentially weighted moving average (EWMA) chart, and generalized T^2 (GT) chart. More examples can be found in [Chen and Nembhard \[1\]](#), [Li et al. \[2\]](#), [Lim and Lee \[3\]](#), [Abdella et al. \[4\]](#), [Wang et al. \[5\]](#), [Yan et al. \[6\]](#), [Feng et al. \[7\]](#), and [Kim et al. \[8\]](#).

Monitoring the variability of high-dimensional processes has two major challenges: (1) the sample covariance matrix is not invertible because its determinant tends to zero, (2) timely reaction to process disturbances is usually impossible since the assignable causes may only affect a tiny number of elements in the covariance matrix. In recent years, few attention has been devoted to development of monitoring schemes for detection of variability disturbances under high-dimensional setting. In this regard, a novel algorithm based on Parallelized Monte Carlo simulation to improve the ability of the multivariate exponentially weighted mean squared deviation and multivariate exponentially weighted moving variance charts to monitor high-dimensional process variability was introduced by [Gunaratne et al. \[9\]](#). [Abdella et al. \[10\]](#) introduced an adaptive LASSO-thresholding-based control chart for monitoring high-dimensional process variability without need of computing the inverse of sample covariance matrix. They highlighted the efficiency of their proposed control chart using real-life data examples from the semiconductor industry and a milling process. Without sparsity assumption, [Kim et al. \[11\]](#) extended a ridge penalized likelihood ratio (RPLR)-based control chart to recognize covariance matrix changes under high-dimensionality. Under the sparsity conditions, [Abdella et al. \[12\]](#) extended the adaptive LASSO-thresholding-based control chart for Phase I monitoring of high-dimensional process dispersion when the in-control covariance matrix is unknown. They used simulated and real-life examples to investigate the sensitivity of their

suggested chart, named as T-COV, in terms of signal probability metric. Taking the idea of tracking changes in the sparse leading eigenvalue between two covariance matrices, [Fan et al. \[13\]](#) designed a sparse-leading-eigenvalue-driven control chart for Phase I monitoring of high-dimensional process variability. They showed that their proposed control chart works better than L_2 -type and L_∞ -type control charts. [Jafari et al. \[14\]](#) proposed an adaptive thresholding LASSO (ATL) control charting method for Phase II monitoring of high-dimensional covariance matrices by considering the impact of gauge inaccuracy. The performance of control chart can be severely dependent on sampling strategies specially when even small delays in detection of assignable causes imposes significant cost on the production system. In this regard, novel sampling strategies such as multiple sampling (MS), ranked set sampling (RSS), multiple dependent state (MDS) sampling and repetitive sampling (RS) have been introduced in the literature to enhance the sensitivity of different control charts. Interested readers are referred to important references such as [Maleki et al. \[15\]](#) and [Maleki et al. \[16\]](#) for MS-based charts, [Salmasnia et al. \[17\]](#), [Khalafi et al. \[18\]](#), and [Nawaz and Han \[19\]](#) for RSS based charts, and finally [Saghir et al. \[20\]](#) and [Shaheen et al. \[21\]](#) for RS-based ones. In recent years, multiple dependent sampling schemes has been successfully employed for further improving of control chart detectability. It can be concluded from the relevant literature that the *MDS* sampling schemes can dominate the other prevalent single sampling (SS) strategies. By employing *MDS* sampling strategies, the null hypothesis of in-control process condition can be (1) accepted, (b) rejected (c) conditionally accepted/rejected. In this regard, [Aslam et al. \[22\]](#) incorporated variable sample size (VSS) and *MDS* strategies for Phase II monitoring of process mean. An adaptive np control chart equipped by *MDS* sampling scheme was introduced by [Zhou et al. \[23\]](#). [Arshad et al. \[24\]](#) employed the *MDS* strategy for Phase II monitoring of process variability. On the basis of *MDS* sampling strategy, [Naveed et al. \[25\]](#) proposed an EWMA-based control chart to detect sustained mean shifts when the quality characteristic of interest follows a normal distribution. [García-Bustos et al. \[26\]](#) focused on Phase II monitoring of correlated Poisson variables based on *MDS* sampling scheme. [Aslam et al. \[27\]](#) employed repetitive group and *MDS* sampling approaches based on the EWMA yield index for product acceptance.

Since the sample covariance matrix is not positive semi-definite when the number of variables goes beyond the sample size, typical control charts established based on the inverse of sample covariance matrix are not applicable. Hence, this paper proposes an improved RPLR chart based

on the generalized multiple dependent state (*GMDS*) sampling strategy here after called *GMDS-RPLR* chart. The developed chart can effectively detect different types of sustained shift in covariance matrix elements without sparsity assumption.

The rest of this paper is organized as follows: the developed control chart is introduced in [Section 2](#). Extensive simulations in terms of the average run length (*ARL*) and standard deviation of run length (*SDRL*) are carried out to evaluate the detectability of the developed chart in [Section 3](#). In [Section 4](#), the sensitivity of the *GMDS-RPLR* chart to the process dimension and repetition parameter is studied. Ultimately, conclusion remarks and future research directions are given in [Section 5](#).

2. Proposed monitoring scheme

As previously mentioned, high-dimensional settings pose new challenges to the conventional multivariate control charts due to the curse of dimensionality. As an efficient monitoring scheme, the ridge penalized likelihood ratio (*RPLR*) can be efficiently used to recognize out-of-control covariance matrix patterns without sparsity condition. On the other hand, the sensitivity of control charts to identify process faults can be increased by using a proper sampling strategy. Hence, this study develops a novel control chart for monitoring high-dimensional covariance matrix by combining *RPLR* statistic with *MDS* sampling strategy hereafter called *MDS-RPLR* chart. A generalized version of *MDS* sampling strategy, called *GMDS*, is also incorporated to establish the chart statistic, named as *GMDS-RPLR*, for further improvement of chart detectability. The notations used to establish the *MDS-RPLR* and *GMDS-RPLR* statistics are given in [Table 1](#).

[Please insert Table 1 about here]

Let $\mathbf{X}_t = (\mathbf{x}_{t1}, \mathbf{x}_{t2}, \dots, \mathbf{x}_{tm})_{p \times n}; t = 1, 2, \dots, T$ be a $p \times n$ matrix of observations collected at sampling point t in which $\mathbf{x}_{ii} = (x_{ii1}, x_{ii2}, \dots, x_{iip})^T; i = 1, \dots, n$ denotes the i^{th} observation of matrix \mathbf{X}_t . It is also assumed that quality trait \mathbf{x}_{ii} follows a multivariate normal distribution with mean vector $\boldsymbol{\mu}$ and covariance matrix $\boldsymbol{\Sigma}_{in}$ when the process is operating in its in-control state. Therefore, the likelihood function of observations $\mathbf{x}_{t1}, \mathbf{x}_{t2}, \dots, \mathbf{x}_{tm}$ can be written as:

$$f(\mathbf{x}_{i1}, \dots, \mathbf{x}_{in} | \mathbf{\Omega}) = (2\pi n)^{\frac{-p}{2}} |\mathbf{\Omega}|^{\frac{1}{2}} e^{-\sum_{i=1}^n (\mathbf{x}_{ii} - \boldsymbol{\mu})^T \mathbf{\Omega} (\mathbf{x}_{ii} - \boldsymbol{\mu})} \quad (1)$$

where $\mathbf{\Omega} = \boldsymbol{\Sigma}^{-1}$ termed as precision matrix denotes the inverse of process covariance matrix. Estimation of the precision matrix by maximum likelihood estimator (MLE) is obtained as Equation (2). The MLE estimates the unknown parameters of a given probability distribution by maximizing a likelihood function in a way that the sampled observations are most probable.

$$\hat{\mathbf{\Omega}}_t^{MLE} = \arg \min_{\mathbf{\Omega}} \{tr(\mathbf{\Omega} \mathbf{S}_t) - \log |\mathbf{\Omega}|\} \quad (2)$$

where $\mathbf{S}_t = \frac{1}{n} \sum_{i=1}^n (\mathbf{x}_{ii} - \boldsymbol{\mu})(\mathbf{x}_{ii} - \boldsymbol{\mu})^T$ represents the sample covariance matrix at sampling point t . It

can be statistically checked that $\hat{\mathbf{\Omega}}_t^{MLE} = \mathbf{S}_t^{-1}$ when the process dimension is smaller than the sample size. However, it is impossible to estimate the precision matrix by MLE under high-dimensional setting because the sample covariance matrix is not invertible. By taking the idea of adding a penalty term to Equation (2), the estimation of precision matrix by the ridge penalized likelihood ratio (*RPLR*) method is given as:

$$\hat{\mathbf{\Omega}}_t^{RPLR} = \arg \min_{\mathbf{\Omega}} \left\{ tr(\mathbf{\Omega} \mathbf{S}_t) - \log |\mathbf{\Omega}| + \frac{\theta}{2} \|\mathbf{\Omega} - \mathbf{\Omega}_{in}\| \right\} \quad (3)$$

where $\mathbf{\Omega}_{in} = \boldsymbol{\Sigma}_{in}^{-1}$ and $\theta; \theta > 0$ is a tuning parameter which is employed to obtain various levels of shrinkage of $\hat{\mathbf{\Omega}}_t^{RPLR}$. For the t^{th} taken sample, Equation (4) represents a closed-form to estimate the precision matrix based on Equation (3):

$$\hat{\mathbf{\Omega}}_t^{RPLR} = \left\{ \left(\theta \mathbf{I}_p + \frac{1}{4} (\mathbf{S}_t - \theta \mathbf{\Omega}_{in})^2 \right)^{\frac{1}{2}} + \frac{1}{2} (\mathbf{S}_t - \theta \mathbf{\Omega}_{in}) \right\}^{-1} \quad (4)$$

It can be concluded from Equation (4) that $\hat{\mathbf{\Omega}}_t^{RPLR}$ tends toward $\mathbf{\Omega}_{in}$ when $\theta \rightarrow \infty$ while in situation that $\theta \rightarrow 0$, $\hat{\mathbf{\Omega}}_t^{RPLR}$ approaches \mathbf{S}_t^{-1} . Alerting an out-of-control signal is equivalent to rejection of null hypothesis $H_0 : \boldsymbol{\Sigma} = \boldsymbol{\Sigma}_{in}$ versus the alternative hypothesis $H_1 : \boldsymbol{\Sigma} \neq \boldsymbol{\Sigma}_{in}$. At the t^{th} sampling point, the developed *GMDS-RPLR* control charting method for Phase II monitoring of high-dimensional process variability uses the following formula:

$$RPLR_t = tr(\mathbf{\Omega}_{in} \mathbf{S}_t) + \ln |\hat{\mathbf{\Omega}}_t^{RPLR}| - \ln |\mathbf{\Omega}_{in}| - tr(\hat{\mathbf{\Omega}}_t^{RPLR} \mathbf{S}_t) \quad (5)$$

According to Equation (5), ideally, i.e. when the estimated precision matrix ($\hat{\Omega}_t^{RPLR}$) is equal to the in-control precision matrix (Ω_{in}), the $RPLR_t$ will be zero. As $\hat{\Omega}_t^{RPLR}$ deviates from its target Ω_{in} , the value of plotting statistic $RPLR_t$ increases. That is to say, the $RPLR_t$ chart statistic will be always greater than or equal to zero. Consequently, the control charting method only requires the upper control limit to evaluate the process variability status. As can be seen in Figure 1, the feasible space for *GMDS-RPLR* control charting scheme can be partitioned into three regions of in-control, out-of-control, and warning. To establish the developed *GMDS-RPLR* control chart, first four parameters ($r, q, UCL_{inner}, UCL_{outer}$); $UCL_{inner} < UCL_{outer}, q \leq r$ are determined such that a pre-determined value for ARL_{in} is obtained.

[Please insert Figure 1 about here]

The process variability condition by *GMDS-RPLR* chart is specified as below:

- 1- The process variability will be deemed in-control when the chart statistic is smaller than or equal to UCL_{inner} .
- 2- The control chart issues an out-of-control signal whenever the *GMDS-RPLR* statistic exceeds UCL_{outer} .
- 3- r additional samples are taken in situation that the *GMDS-RPLR* statistic falls within the warning region ($UCL_{inner} < GMDS - RPLR_t < UCL_{outer}$). In this case, the process is deemed in-control if and only if both two following conditions are satisfied: (1) the chart statistic for at least q out of r samples falls within the in-control region; (2) The chart statistic corresponding to the remaining samples do not exceed UCL_{outer} . In contrast, the *GMDS-RPLR* triggers an out-of-control alert even if one of the mentioned conditions is violated. For more clarification, the *GMDS-RPLR* monitoring scheme is illustrated in Figure 2.

[Please insert Figure 2 about here]

3. Performance evaluation of *MDS-RPLR* and *GMDS-RPLR* monitoring schemes

In this section, seven out-of-control patterns are taken into consideration to evaluate the run length properties of the developed *MDS-RPLR* and *GMDS-RPLR* monitoring schemes. Note that, run length is a geometric random variable which is defined as the number of plotted samples taken from the process until the first plotting statistic falls within the out-of-control region. The in-control covariance matrix is considered as $\Sigma_{in} = \mathbf{I}_p$ and the process dimension is selected as $p = 10$.

The out-of-control patterns involve three general structures: (1) diagonal shifts; (2) off-diagonal shifts; and (3) joint diagonal and off-diagonal shifts. For each out-of-control pattern, it is assumed that when the covariance matrix deviates from \mathbf{I}_p to $\Sigma_{out,l}; l = 1, \dots, 7$, the occurred change remains until issuing an out-of-control signal by the control chart. In rest, each pattern is explained in detail.

Pattern 1: According to Equation 6, under this pattern, the diagonal elements deviate from 1 to $1 + \Delta^2$ while the values of off-diagonal elements increase from 0 to Δ .

$$\Sigma_{out,1} = \begin{bmatrix} 1 + \Delta^2 & \Delta & \dots & \Delta \\ \Delta & 1 + \Delta^2 & \dots & \Delta \\ \vdots & \vdots & \ddots & \vdots \\ \Delta & \Delta & \dots & 1 + \Delta^2 \end{bmatrix}_{10 \times 10} \quad (6)$$

Pattern 2: This pattern is similar to the previous pattern with this difference that the diagonal and off-diagonal elements related to first five quality characteristics are affected by the assignable cause.

$$\Sigma_{out,2} = \begin{bmatrix} 1 + \Delta^2 & \Delta & \dots & \Delta & 0 & \dots & 0 \\ \Delta & 1 + \Delta^2 & \dots & \Delta & 0 & \dots & 0 \\ \vdots & \vdots & \ddots & \Delta & \vdots & \dots & \vdots \\ \Delta & \Delta & \dots & 1 + \Delta^2 & 0 & \dots & 0 \\ 0 & 0 & \dots & 0 & 1 & \dots & 0 \\ \vdots & \vdots & \vdots & \vdots & \vdots & \ddots & \vdots \\ 0 & 0 & \dots & 0 & 0 & \dots & 1 \end{bmatrix}_{10 \times 10} \quad (7)$$

Pattern 3: Similar to the previous out-of-control scenarios, this pattern belongs to the third mentioned out-of-control structure where the assignable cause affects the variance and covariance of the first and second variables.

$$\Sigma_{out,3} = \begin{bmatrix} \boxed{1+\Delta^2} & \Delta & 0 & \dots & 0 \\ \Delta & \boxed{1+\Delta^2} & 0 & \dots & 0 \\ 0 & 0 & 1 & \dots & 0 \\ \vdots & \vdots & \vdots & \ddots & \vdots \\ 0 & 0 & 0 & \dots & 1 \end{bmatrix}_{10 \times 10} \quad (8)$$

Pattern 4: Under this pattern, the occurrence of assignable cause only changes the variance elements while the covariances remain unchanged.

$$\Sigma_{out,4} = \begin{bmatrix} 1+\Delta^2 & 0 & \dots & 0 \\ 0 & 1+\Delta^2 & \dots & 0 \\ \vdots & \vdots & \ddots & \vdots \\ 0 & 0 & \dots & 1+\Delta^2 \end{bmatrix}_{10 \times 10} \quad (9)$$

Pattern 5: Only the variance of the first variable among all covariance matrix elements deviates from its nominal value under the occurrence of the assignable cause.

$$\Sigma_{out,5} = \begin{bmatrix} 1+\Delta^2 & 0 & \dots & 0 \\ 0 & 1 & \dots & 0 \\ \vdots & \vdots & \ddots & \vdots \\ 0 & 0 & \dots & 1 \end{bmatrix}_{10 \times 10} \quad (10)$$

Pattern 6: This pattern is related to the second out-of-control structure in which only the off-diagonal elements corresponding to the first five quality characteristics increase Δ units.

$$\Sigma_{out,6} = \begin{bmatrix} 1 & \Delta & \cdots & \Delta & 0 & \cdots & 0 \\ \Delta & 1 & \cdots & \Delta & 0 & \cdots & 0 \\ \vdots & \vdots & \ddots & \vdots & \vdots & \cdots & \vdots \\ \Delta & \Delta & \cdots & 1 & 0 & \cdots & 0 \\ 0 & 0 & \cdots & 0 & 1 & \cdots & 0 \\ \vdots & \vdots & \vdots & \vdots & \vdots & \ddots & \vdots \\ 0 & 0 & \cdots & 0 & 0 & \cdots & 1 \end{bmatrix}_{10 \times 10} \quad (11)$$

Pattern 7: This pattern is similar to the latter mentioned one except that only the covariance between the first and second variables is affected when the assignable cause occurs.

$$\Sigma_{out,7} = \begin{bmatrix} 1 & \Delta & 0 & \cdots & 0 \\ \Delta & 1 & 0 & \cdots & 0 \\ 0 & 0 & 1 & \cdots & 0 \\ \vdots & \vdots & \vdots & \ddots & \vdots \\ 0 & 0 & 0 & \cdots & 1 \end{bmatrix}_{10 \times 10} \quad (12)$$

In simulations, the sample size is set at $n = 5$ and the tuning parameter of the developed charts is fixed at $\theta = 10$. The process mean is supposed to be a zero vector with size 10×1 . Moreover, the repetition parameter of the *MDS-RPLR* and *GMDS-RPLR* charts is considered as $r = 3$ while two values of $q \in \{1, 2\}$ are used for the generalization parameter. To have fair comparisons, the values of control limits for the competing charts are calibrated such that $ARL_{in} = 200$ which is equivalent to probability of Type I error $\alpha = 0.005$. It is remarkable that the probability of Type I error means rejecting the null hypothesis that the process is statistically in-control in condition that it's actually true. Then, the sensitivity of the developed charts under the defined out-of-control patterns are compared by considering different shift magnitudes $\Delta \in \{0, 0.1, 0.2, 0.3, 0.5, 0.75, 1\}$. Obviously, the condition $\Delta = 0$ implies that all covariance matrix elements remain in-control. The detectability of the *RPLR*, *MDS-RPLR* and *GMDS-RPLR* monitoring schemes in terms of the *ARL* and *SDRL* metrics under the mentioned out-of-control patterns are compared in [Tables 2-8](#). Note that, the resulting *ARLs* and *SDRLs* are extracted based on 10000 simulation replicates in MATLAB program.

It can be observed from Tables 2-8 that for all shift magnitudes, the *MDS-RPLR* control charting method outperforms the *RPLR* scheme in detecting all out-of-control patterns. In other words, employing *MDS* strategy significantly enhances the sensitivity of the *RPLR* control chart. For example under out-of-control pattern 1 as a joint diagonal/off-diagonal structure, the out-of-control *ARLs* for *RPLR* are obtained as 71.808, 18.923, 7.931, 3.208, 1.776, and 1.303 for shift magnitudes 0.1, 0.2, 0.3, 0.5, 0.75, and 1, respectively. However, the obtained *ARLs* for the *GMDS-RPLR* chart under the mentioned conditions are 67.751, 14.509, 5.515, 1.820, 1.135, and 1.017. That is to say for $\Delta = 0.1, 0.2, 0.3, 0.5, 0.75, 1$, the *MDS-RPLR* chart performs about 5.65%, 23.33%, 30.46%, 43.27%, 36.09%, and 21.95% better than the *RPLR* one. Under pattern 4 in which only diagonal elements deviate from their nominal values, the *RPLR* chart gives $ARL=181.337, 112.376, 61.302, 13.481, 2.745, \text{ and } 1.263$ for $\Delta = 0.1, 0.2, 0.3, 0.5, 0.75, 1$ whereas for the *MDS-RPLR* chart we have $ARL=170.878, 104.994, 47.655, 6.730, 1.166, \text{ and } 1.002$. It means that under the mentioned shift magnitudes, the *MDS-RPLR* chart performs about 5.77%, 6.57%, 22.26%, 50.08%, 57.52%, and 20.66 % better than the *RPLR* one. Finally, in pattern 6 which belongs to the off-diagonal out-of-control structure, the *ARL* for the *RPLR* chart are obtained as 161.569, 92.949, 47.315, 16.919, 7.912, and 4.811 under the considered shift magnitudes. The *ARL* values decrease to 154.091, 82.466, 41.355, 14.390, 5.745, and 3.096 when the *MDS-RPLR* chart is used for monitoring the process variability. These values confirm 4.31%, 9.09%, 41.35%, 14.39%, 5.74%, and 28.27% reduction in *ARL* values when employing the *MDS-RPLR* chart instead of the *RPLR* one. Moreover, considering all seven out-of-control patterns, it can be concluded that the superiority of the *MDS-RPLR* chart over the competing *RPLR* chart is more tangible under large shift magnitudes. As another important conclusion, it can be seen that for all diagonal, off-diagonal and joint diagonal/off-diagonal out-of-control structures, the improvement percentage increases as the number of shifted elements increase when the *MDS* scheme is utilized. Similar conclusions can be drawn when taking *SDRL* into consideration.

Since the *GMDS* strategy is more flexible than the simple random and *MDS* sampling strategies, we anticipate to get far better results from *GMDS-RPLR* chart than the competing *RPLR* and *MDS-RPLR* ones. As expected, in comparison with *RPLR* and *MDS-RPLR* charts, the *GMDS-RPLR* gains higher detection power under all seven out-of-control shift patterns. However, the superiority of the *GMDS-RPLR* chart over the *MDS-RPLR* one is less than that of *MDS-RPLR*

chart over *RPLR* monitoring scheme. For instance under pattern 1, the sensitivity of the *GMDS-RPLR* chart for $q=1$ and $q=2$ is averagely about 12.01% and 11.69% more than the *MDS-RPLR* scheme while the average improvement percentage of the *MDS-RPLR* chart over the *RPLR* scheme is 26.79. As seen, for off-diagonal shift structure, i.e., patterns 6 and 7, selecting $q=1$ for the *GMDS-RPLR* monitoring scheme leads to smaller *ARLs* and *SDRLs* than $q=2$. However, for both diagonal and joint sustained shifts, i.e., patterns 1-5, the setting the generalization parameter at $q=2$ results in better performance of the *GMDS-RPLR* chart in reacting to large shift magnitudes. In contrast, designing the *GMDS-RPLR* by choosing $q=1$ increases its detection capability to recognize small and moderate shift magnitudes.

[Please insert Tables 2-8 about here]

4. Sensitivity Analysis

In this section, a sensitivity analysis is carried out to explore how the process dimension and the repetition parameter affect the detectability of the proposed control charts. Note that, sensitivity analysis is a technique that determines how different values of an independent variable can impact a dependent variable under a given set of assumptions. For this purpose, we focus on out-of-control pattern 1 and consider the same parameter values used in the previous section. In addition, three values of $p=10,12,15$ and $r=3,4,5$ are selected for process dimension and repetition parameter, respectively. The *ARLs* and *SDRLs* of the developed control charts for different process dimension values when $r=3$ are reported in Table 9. As can be seen, the detection capability of four competing control charts improves as the number of variables increases. As instance, we have $ARL=18.923$ under $\Delta=0.2$ for *RPLR* control chart when $p=10$ whereas the *ARL* value decreases to 15.064 and 13.424 in cases of $p=12$ and 15. Under the mention condition, the *ARL* reduces from 14.509 to 9.365 and 4.003 when employing *MDS-RPLR* chart. Finally, for *GMDS-RPLR* chart (case $q=1$), increasing the number of variables from 10 to 12 and 15 leads to decreasing the *ARL* value from 11.476 to 6.674 and 2.727, respectively. As another important finding, it can be concluded that the most tangible *ARL* improvement percentage belongs to *GMDS-RPLR* chart while increasing the process dimension has the least effect on detectability of the *RPLR* monitoring scheme. For example, under $\Delta=0.2$ the *ARL* improvement percentage of *RPLR*, *MDS-RPLR* and *GMDS-RPLR* for $q=1$ are about

20.39%, 35.45%, and 41.84%, respectively when p increases from 10 to 12. However, a reverse trend can be seen when $\Delta = 1$ because the ARL values of $MDS-RPLR$ and $GMDS-RPLR$ charts under this shift magnitude are very close to 1 even for $p = 10$. Furthermore, the ARL improvement for all competing control charts is more significant when $\Delta \in \{0.2, 0.3\}$. Similar results can be observed when the $SDRL$ metric is taken into account.

The sensitivity of the developed control charts to repetition parameter is evaluated and the resulting ARL and $SDRL$ values are given in Table 10. As seen, the power of the developed charts enhances with selecting larger values of r . However, the detection ability of the developed monitoring schemes is not significantly dependent on the value of repetition parameter. In other words, it seems that taking $r = 3$ additional samples will be adequate when the chart statistics falls within the warning region.

[Please insert Tables 9-10 about here]

5. Conclusion

In today's highly competitive industrial society, companies are considering more quality attributes in order to fulfil their increasing customer expectations. Consequently, this problem highlights the necessity of developing control charts for monitoring high-dimensional data streams. In this context, a novel monitoring scheme called $MDS-RPLR$ based on the integration of the multiple dependent state sampling strategy and the ridge penalized likelihood ratio statistic was developed. Then, in order to enhance the flexibility of the developed $MDS-RPLR$ chart, a generalized version of the MDS strategy was suggested to establish the plotting statistic of the $RPLR$ chart named $GMDS-RPLR$ monitoring scheme. Extensive comparative studies based on Mont Carlo simulations were carried out to compare the run length properties of the developed charts in terms of ARL and $SDRL$ metrics. The obtained results confirmed that under three general diagonal, off-diagonal as well as joint diagonal/off-diagonal out-of-control structures, the $GMDS-RPLR$ chart works better than both $RPLR$ and $MDS-RPLR$. However, the superiority of the $GMDS-RPLR$ monitoring scheme over the $MDS-RPLR$ chart is less tangible than that of the $MDS-RPLR$ chart over $RPLR$ one. The results of sensitivity analysis showed that the reaction capability of the developed charts to sustained shift in covariance matrix elements improves as the process dimension increases. However, the performance of the developed charts

is not much dependent to the value of repetition parameter. While this study focused on monitoring of high-dimensional process variability, future research directions can look into simultaneous monitoring of mean vector and covariance matrix of high-dimensional data streams. Extending nonparametric control charts for monitoring high-dimensional covariance matrices can be also a fruitful area as a future direction.

References

1. Chen, S., and Nembhard, H. B. "A high- dimensional control chart for profile monitoring", *Quality and Reliability Engineering International*, **27**(4), pp. 451-464 (2011).
2. Li, Y., Liu, Y., Zou, C., et al. "A self-starting control chart for high-dimensional short-run processes", *International Journal of Production Research*, **52**(2), pp. 445-461 (2014).
3. Lim, J., and Lee, S. "Phase II monitoring of changes in mean from high- dimensional data", *Applied Stochastic Models in Business and Industry*, **33**(6), pp. 626-639 (2017).
4. Abdella, G. M., Al- Khalifa, K. N., Kim, S., et al. "Variable selection- based multivariate cumulative sum control chart", *Quality and Reliability Engineering International*, **33**(3), pp. 565-578 (2017).
5. Wang, Z., Li, Y., and Zhou, X. "A statistical control chart for monitoring high- dimensional Poisson data streams", *Quality and Reliability Engineering International*, **33**(2), pp. 307-321 (2017).
6. Yan, D., Zhang, S., and Jung, U. "A variable- selection control chart via penalized likelihood and Gaussian mixture model for multimodal and high- dimensional processes", *Quality and Reliability Engineering International*, **35**(4), pp. 1263-1275 (2019).
7. Feng, L., Ren, H., and Zou, C. "A setwise EWMA scheme for monitoring high-dimensional datastreams", *Random Matrices: Theory and Applications*, **9**(02), 2050004 (2020).
8. Kim, S., Jeong, M. K., and Elsayed, E. A. "A penalized likelihood-based quality monitoring via L2- norm regularization for high-dimensional processes", *Journal of Quality Technology*, **52**(3), pp. 265-280 (2020).
9. Gunaratne, N. G. T., Abdollahian, M. A., Huda, S., et al. "Exponentially weighted control charts to monitor multivariate process variability for high dimensions", *International Journal of Production Research*, **55**(17), pp. 4948-4962 (2017)..
10. Abdella, G. M., Kim, J., Kim, S., et al. "An adaptive thresholding-based process variability monitoring", *Journal of Quality Technology*, **51**(3), pp. 242-256 (2019).
11. Kim, J., Abdella, G. M., Kim, S., et al. "Control charts for variability monitoring in high- dimensional processes", *Computers & Industrial Engineering*, **130**, pp. 309-316 (2019).

12. Abdella, G. M., Maleki, M. R., Kim, S., et al. "Phase-I monitoring of high-dimensional covariance matrix using an adaptive thresholding LASSO rule", *Computers & Industrial Engineering*, **144**, 106465 (2020).
13. Fan, J., Shu, L., Yang, A., et al. "Phase I analysis of high-dimensional covariance matrices based on sparse leading eigenvalues", *Journal of Quality Technology*, **53**(4), pp. 333-346 (2021).
14. Jafari, M., Maleki, M. R., and Salmasnia, A. "A high-dimensional control chart for monitoring process variability under gauge imprecision effect", *Production Engineering*, In Press (2022).
15. Maleki, M. R., Shamseddin, B., Eghbali, H., et al. "The effect of gauge measurement errors on double sampling \bar{X} control chart", *Communications in Statistics-Theory and Methods*, DOI: 10.1080/03610926.2021.1958848 (2022a).
16. Maleki, M. R., Salmasnia, A., and Yarmohammadi Saber, S. "The Performance of Triple Sampling \bar{X} Control Chart with Measurement Errors", *Quality Technology & Quantitative Management*, **19**(5), pp. 587-604 (2022b)..
17. Salmasnia, A., Maleki, M. R., and Niaki, S. T. A. "Remedial measures to lessen the effect of imprecise measurement with linearly increasing variance on the performance of the MAX-EWMAMS scheme", *Arabian Journal for Science and Engineering*, **43**(6), pp. 3151-3162 (2018).
18. Khalafi, S., Salmasnia, A., and Maleki, M. R. "Remedial approaches to decrease the effect of measurement errors on simple linear profile monitoring", *International Journal for Quality Research*, **14**(4), 1019 (2020).
19. Nawaz, T., and Han, D. "Monitoring the process location by using new ranked set sampling-based memory control charts", *Quality Technology & Quantitative Management*, **17**(3), pp. 255-284 (2020)..
20. Saghir, A., Ahmad, L., Aslam, M., et al. "A EWMA control chart based on an auxiliary variable and repetitive sampling for monitoring process location", *Communications in Statistics-Simulation and Computation*, **48**(7), pp. 2034-2045 (2019).
21. Shaheen, U., Azam, M., and Aslam, M. "A control chart for monitoring the lognormal process variation using repetitive sampling", *Quality and Reliability Engineering International*, **36**(3), pp. 1028-1047 (2020).
22. Aslam, M., Arif, O. H., and Jun, C. H. "A new variable sample size control chart using MDS sampling", *Journal of Statistical Computation and Simulation*, **86**(18), pp. 3620-3628 (2016).
23. Zhou, W., Wan, Q., Zheng, Y., et al. "A joint-adaptive np control chart with multiple dependent state sampling scheme", *Communications in Statistics-Theory and Methods*, **46**(14), pp. 6967-6979 (2017).
24. Arshad, A., Azam, M., Aslam, M., et al. "A control chart for monitoring process variation using multiple dependent state sampling", *Communications in Statistics-Simulation and Computation*, **47**(8), pp. 2216-2233 (2018).

25. Naveed, M., Azam, M., Khan, N., et al. "Designing a control chart of extended EWMA statistic based on multiple dependent state sampling", *Journal of Applied Statistics*, **47**(8), pp. 1482-1492 (2020).
26. García-Bustos, S., Plaza, A., and Cárdenas-Escobar, N. "An optimal multivariate control chart for correlated Poisson variables using multiple dependent state sampling", *Production Engineering*, **16**, pp. 145-155 (2021)..
27. Aslam, M., Azam, M., Sherwani, R. A. K., et al. "Product acceptance determination based on EWMA yield index using repetitive and MDS sampling schemes", *Scientia Iranica*, **29**(4), pp. 2241-2251 (2022).

Biographies

Maziar Saemian is a Ph.D candidate of Industrial Engineering at the University of Eyvanekey in Iran. He has obtained his B.S in Mechanical Engineering from the Islamic Azad University, Abhar Branch in Iran. He also received his M.S degree in Industrial Engineering from Khatam University. His research interests are statistical process monitoring and data analysis.

Ali Salmasnia is currently an Associate Professor at the University of Qom, Qom, Iran. His research interests include statistical process monitoring, reliability engineering, cloud manufacturing, and data analysis. He is the author or co-author of various papers published in *Journal of Manufacturing Systems*, *Computers & Industrial Engineering*, *Applied Soft Computing*, *Neurocomputing*, *Applied Mathematical Modelling*, *Expert Systems with Applications*, *Quality Technology & Quantitative Management*, *Journal of Information Science*, *Neural Computing & Applications*, *Applied Stochastic Models in Business and Industry*, *IEEE Transactions on Engineering Management*, *International Journal of Information Technology & Decision Making*, *Operational Research*, *TOP*, *Quality and Reliability Engineering International*, *Journal of Statistical Computation and Simulation*, *International Journal of Advanced Manufacturing Technology*, *Communications in Statistics - Simulation and Computation*, *Arabian Journal for Science and Engineering* and *Scientia Iranica*.

Mohammad Reza Maleki is currently an Assistant Professor at the Golpayegan College of Engineering in Isfahan University of Technology. His research interests include statistical process monitoring, reliability engineering, and data analysis. He has been the author or co-author of many papers published in high-ranked journals such as *Computers & Industrial Engineering*, *Quality Technology & Quantitative Management*, *Quality and Reliability Engineering International*, *Journal of Statistical Computation and Simulation*, *Communications in Statistics - Simulation and Computation*, *Communications in Statistics -*

Theory and Methods, Transactions of the Institute of Measurement and Control, Journal of Industrial and Business Economics, Arabian Journal for Science and Engineering, and Scientia Iranica.

Figures

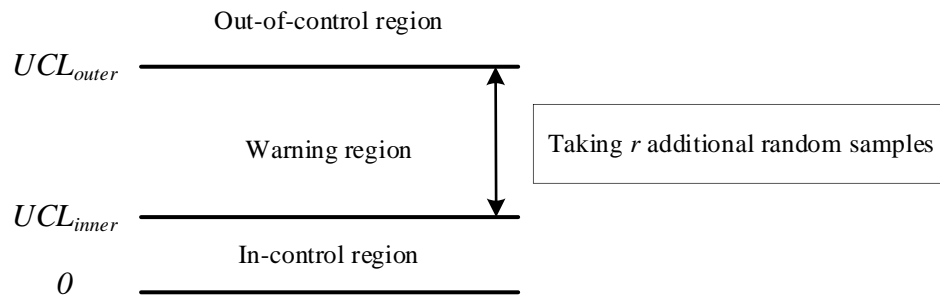


Figure 1. Graphical view of GMDS-RPLR chart

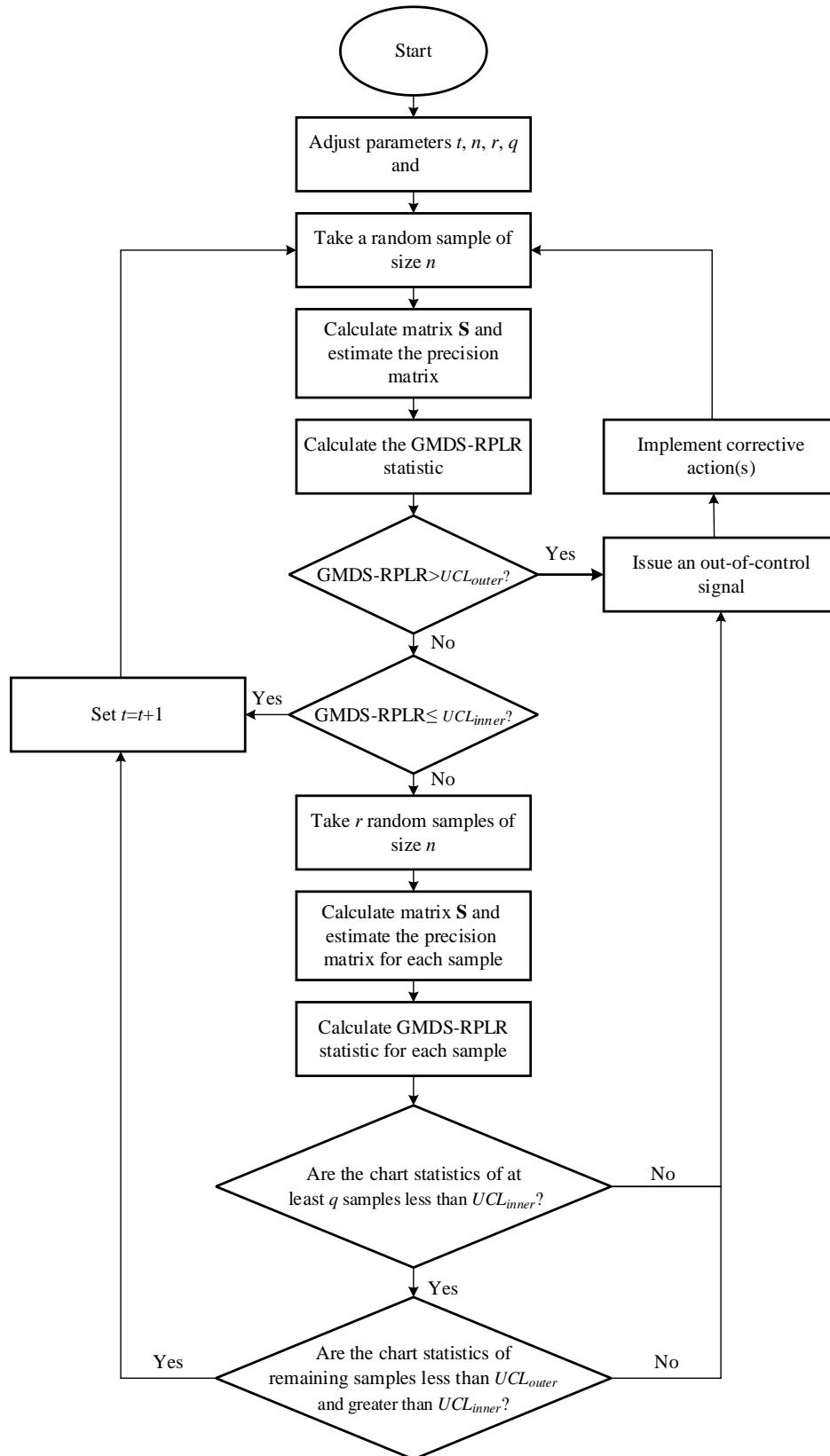


Figure 2. GMDS-RPLR monitoring scheme

Tables

Table 1. Notations

Notation	Description
Indices	
t	Index of subgroups
i	Index of observations
j, k	Indices of variables
l	Index of out-of-control scenario
Distribution parameters	
\mathbf{X}_t	Matrix of observations in subgroup t
\mathbf{x}_{ti}	The i^{th} observation in subgroup t
x_{ijk}	The i^{th} observation from j^{th} variable in subgroup t
p	Number of variables
$\boldsymbol{\mu}$	Mean vector of \mathbf{X}_t
$\boldsymbol{\Sigma}$	Covariance matrix of \mathbf{X}_t
$\boldsymbol{\Omega}$	Precision matrix of \mathbf{X}_t
$\boldsymbol{\Sigma}_{in}$	In-control covariance matrix of \mathbf{X}_t
$\boldsymbol{\Omega}_{in}$	In-control precision matrix of \mathbf{X}_t
$\boldsymbol{\Sigma}_{out,l}$	Out-of-control covariance matrix of \mathbf{X}_t under pattern l
σ_{jk}	Covariance of quality characteristics j and k
σ_j^2	Variance of j^{th} quality characteristic
Chart parameters	
α	Probability of Type I error
n	Sample size
θ	Tuning parameter of <i>RPLR</i> chart
r	Repetition parameter of <i>MDS-RPLR</i> and <i>GMDS-RPLR</i> charts
q	Generalization parameter of <i>GMDS-RPLR</i> chart
UCL	Upper control limit of <i>RPLR</i> chart
UCL_{inner}	Inner control limit of <i>MDS-RPLR</i> and <i>GMDS-RPLR</i> charts
UCL_{outer}	Outer control limit of <i>MDS-RPLR</i> and <i>GMDS-RPLR</i> charts
Sample parameters	
\mathbf{S}_t	Sample covariance matrix of subgroup t
$\hat{\boldsymbol{\Omega}}_t^{MLE}$	Estimated precision matrix of \mathbf{X}_t obtained by MLE
$\hat{\boldsymbol{\Omega}}_t^{RPLR}$	Estimated precision matrix of \mathbf{X}_t based on <i>RPLR</i> method
Others	
ARL_{in}	In-control average run length

ARL_{out}	Out-of-control average run length
$SDRL_{in}$	In-control standard deviation of run length
$SDRL_{out}$	Out-of-control standard deviation of run length
T	Signal point

Table 2. ARL and SDRL comparison of the proposed RPLR charts when $n = 5$ and $p = 10$ under pattern 1

Control chart		(CL_{inner}, CL_{outer})	Criterion	Δ						
				0	0.1	0.2	0.3	0.5	0.75	1
RPLR		(4.8104, 4.8104)	ARL	200.027	71.808	18.923	7.931	3.208	1.776	1.303
			SDRL	198.376	69.230	18.508	7.544	2.698	1.228	0.617
MDS-RPLR		(2.2204, 4.8704)	ARL	200.134	67.751	14.509	5.515	1.820	1.135	1.017
			SDRL	200.326	68.836	15.338	5.310	1.444	0.445	0.133
GMDS-RPLR	$q = 1$	(1.7104, 5.0618)	ARL	201.012	60.471	11.476	4.365	1.559	1.088	1.006
			SDRL	198.339	60.255	11.687	4.091	1.006	0.333	0.080
	$q = 2$	(1.2978, 5.1149)	ARL	199.675	60.001	12.261	4.502	1.534	1.048	1.002
			SDRL	201.477	60.180	12.124	4.216	0.976	0.226	0.045

Table 3. ARL and SDRL comparison of the proposed RPLR charts when $n = 5$ and $p = 10$ under pattern 2

Control chart		(CL_{inner}, CL_{outer})	Criterion	Δ						
				0	0.1	0.2	0.3	0.5	0.75	1
RPLR		(4.8104, 4.8104)	ARL	200.027	151.715	73.459	33.272	10.208	3.970	2.288
			SDRL	198.376	156.935	75.545	33.108	9.670	3.342	1.727
MDS-RPLR		(2.2204, 4.8704)	ARL	200.134	148.049	65.119	27.582	6.520	2.217	1.236
			SDRL	200.326	150.226	65.455	27.099	6.432	1.851	0.622
GMDS-RPLR	$q = 1$	(1.7104, 5.0618)	ARL	201.012	136.963	58.848	21.571	4.830	1.643	1.092
			SDRL	198.339	131.278	60.384	21.271	4.412	1.164	0.326
	$q = 2$	(1.2978, 5.1149)	ARL	199.675	136.848	58.846	22.118	4.874	1.572	1.081
			SDRL	201.477	139.800	58.259	22.068	4.518	1.024	0.298

Table 4. ARL and SDRL comparison of the proposed RPLR charts when $n = 5$ and $p = 10$ under pattern 3

Control chart		(CL_{inner}, CL_{outer})	Criterion	Δ						
				0	0.1	0.2	0.3	0.5	0.75	1

<i>RPLR</i>		(4.8104, 4.8104)	<i>ARL</i>	200.027	182.462	167.445	134.455	62.598	23.357	9.100
			<i>SDRL</i>	198.376	177.026	167.155	131.036	64.563	22.793	8.649
<i>MDS-RPLR</i>		(2.2204, 4.8704)	<i>ARL</i>	200.134	181.950	159.491	123.656	52.136	15.580	5.264
			<i>SDRL</i>	200.326	181.314	162.166	122.356	51.736	15.598	5.057
<i>GMDS-RPLR</i>	<i>q</i> = 1	(1.7104, 5.0618)	<i>ARL</i>	201.012	181.274	154.187	115.876	47.129	11.468	3.623
			<i>SDRL</i>	198.339	181.095	153.371	114.529	47.311	10.875	3.309
	<i>q</i> = 2	(1.2978, 5.1149)	<i>ARL</i>	199.675	181.232	155.659	113.928	45.116	11.141	3.319
			<i>SDRL</i>	201.477	181.364	151.671	113.542	44.166	10.836	2.857

Table 5. *ARL* and *SDRL* comparison of the proposed *RPLR* charts when $n = 5$ and $p = 10$ under pattern 4

Control chart		(CL_{inner}, CL_{outer})	Criterion	Δ						
				0	0.1	0.2	0.3	0.5	0.75	1
<i>RPLR</i>		(4.8104, 4.8104)	<i>ARL</i>	200.027	181.337	112.376	61.302	13.481	2.745	1.263
			<i>SDRL</i>	198.377	184.067	111.132	61.022	12.884	2.131	0.563
<i>MDS-RPLR</i>		(2.2204, 4.8704)	<i>ARL</i>	200.134	170.878	104.994	47.655	6.730	1.166	1.002
			<i>SDRL</i>	200.326	171.379	106.227	46.879	6.334	0.459	0.045
<i>GMDS-RPLR</i>	<i>q</i> = 1	(1.7104, 5.0618)	<i>ARL</i>	201.012	168.173	91.858	39.323	4.110	1.063	1.001
			<i>SDRL</i>	198.339	170.265	93.448	39.133	3.655	0.267	0.022
	<i>q</i> = 2	(1.2978, 5.1149)	<i>ARL</i>	199.675	165.674	92.277	37.167	3.524	1.029	1.000
			<i>SDRL</i>	201.477	162.048	92.169	36.498	3.137	0.182	0.000

Table 6. *ARL* and *SDRL* comparison of the proposed *RPLR* charts when $n = 5$ and $p = 10$ under pattern 5

Control chart		(CL_{inner}, CL_{outer})	Criterion	Δ						
				0	0.1	0.2	0.3	0.5	0.75	1
<i>RPLR</i>		(4.8104, 4.8104)	<i>ARL</i>	200.027	193.084	190.507	172.301	131.018	75.203	33.006
			<i>SDRL</i>	198.377	193.381	190.130	172.226	128.416	74.994	32.834
<i>MDS-RPLR</i>		(2.2204, 4.8704)	<i>ARL</i>	200.134	192.345	188.357	169.842	121.438	63.164	25.152
			<i>SDRL</i>	200.326	192.436	190.131	171.748	119.312	62.391	25.341
<i>GMDS-RPLR</i>	<i>q</i> = 1	(1.7104, 5.0618)	<i>ARL</i>	201.012	190.829	180.497	167.599	111.936	51.955	18.500
			<i>SDRL</i>	198.339	187.431	180.195	168.113	110.581	50.927	17.707
	<i>q</i> = 2	(1.2978, 5.1149)	<i>ARL</i>	199.675	191.901	187.972	170.854	115.707	53.788	17.964
			<i>SDRL</i>	201.477	197.941	187.502	172.492	112.134	54.745	18.289

Table 7. ARL and SDRL comparison of the proposed RPLR charts when $n = 5$ and $p = 10$ under pattern 6

Control chart		(CL_{inner}, CL_{outer})	Criterion	Δ						
				0	0.1	0.2	0.3	0.5	0.75	1
RPLR		(4.8104, 4.8104)	ARL	200.027	161.569	92.949	47.315	16.919	7.912	4.811
			SDRL	198.377	161.036	90.715	45.509	16.599	7.487	4.316
MDS-RPLR		(2.2204, 4.8704)	ARL	200.134	154.091	82.466	41.355	14.390	5.745	3.096
			SDRL	200.326	154.672	85.301	41.964	13.860	5.645	2.758
GMDS-RPLR	$q = 1$	(1.7104, 5.0618)	ARL	201.012	147.017	74.417	35.981	11.957	4.541	2.779
			SDRL	198.339	147.463	75.013	36.194	11.964	4.332	2.435
	$q = 2$	(1.2978, 5.1149)	ARL	199.675	153.617	78.258	37.169	12.530	5.029	2.742
			SDRL	201.477	145.162	81.225	38.053	12.283	4.547	2.324

Table 8. ARL and SDRL comparison of the proposed RPLR charts when $n = 5$ and $p = 10$ under pattern 7

Control chart		(CL_{inner}, CL_{outer})	Criterion	Δ						
				0	0.1	0.2	0.3	0.5	0.75	1
RPLR		(4.8104, 4.8104)	ARL	200.027	194.641	186.228	175.723	127.343	80.962	55.976
			SDRL	198.377	194.810	187.822	172.551	124.626	75.271	56.240
MDS-RPLR		(2.2204, 4.8704)	ARL	200.134	193.429	179.471	162.959	117.257	76.503	47.510
			SDRL	200.326	193.537	175.423	159.834	117.244	75.434	48.285
GMDS-RPLR	$q = 1$	(1.7104, 5.0618)	ARL	201.012	191.395	178.856	158.116	116.272	67.556	40.255
			SDRL	198.339	190.157	177.343	159.826	117.869	69.649	41.625
	$q = 2$	(1.2978, 5.1149)	ARL	199.675	195.329	177.741	166.328	118.014	70.161	41.081
			SDRL	201.477	191.979	180.9583	163.042	114.897	71.103	41.720

Table 9. Sensitivity analysis on process dimension under pattern 1 when $r = 3$

Control chart	p	(CL_{inner}, CL_{outer})	Criterion	Δ					
				0.1	0.2	0.3	0.5	0.75	1
RPLR	10	(4.8104, 4.8104)	ARL	71.808	18.923	7.931	3.208	1.776	1.303
			SDRL	69.230	18.508	7.544	2.698	1.228	0.617
	12	(6.1074, 6.1074)	ARL	62.606	15.064	6.687	2.813	1.688	1.275
			SDRL	62.136	14.415	6.107	2.303	1.058	0.607
	15	(8.3142, 8.3142)	ARL	53.780	13.424	5.768	2.523	1.555	1.210
			SDRL	53.295	13.231	5.391	1.993	0.908	0.512

<i>MDS-RPLR</i>		10	(2.2204, 4.8704)	<i>ARL</i>	67.751	14.509	5.515	1.820	1.135	1.017
				<i>SDRL</i>	68.836	15.338	5.310	1.444	0.445	0.133
		12	(2.3104, 6.5315)	<i>ARL</i>	50.613	9.365	3.469	1.412	1.050	1.005
				<i>SDRL</i>	52.263	9.282	3.102	0.863	0.233	0.071
		15	(2.5387, 9.9142)	<i>ARL</i>	26.562	4.003	1.893	1.151	1.015	1.001
				<i>SDRL</i>	26.208	3.510	1.365	0.449	0.133	0.023
<i>GMDS-RPLR</i>	<i>q = 1</i>	10	(1.7104, 5.0618)	<i>ARL</i>	60.471	11.476	4.365	1.559	1.088	1.006
				<i>SDRL</i>	60.255	11.687	4.091	1.006	0.333	0.080
		12	(1.8105, 7.0535)	<i>ARL</i>	39.237	6.674	2.582	1.215	1.023	1.001
				<i>SDRL</i>	40.254	6.057	2.183	0.552	0.167	0.032
		15	(2.1397, 10.7000)	<i>ARL</i>	19.551	2.727	1.468	1.065	1.007	1.001
				<i>SDRL</i>	19.009	2.148	0.849	0.254	0.083	0.031
	<i>q = 2</i>	10	(1.2978, 5.1149)	<i>ARL</i>	60.001	12.261	4.502	1.534	1.048	1.002
				<i>SDRL</i>	60.180	12.124	4.216	0.976	0.226	0.045
		12	(1.4079, 7.2561)	<i>ARL</i>	36.953	6.320	2.402	1.188	1.023	1.001
<i>SDRL</i>	35.904			6.089	1.816	0.476	0.156	0.032		
15	(1.7371, 11.1836)	<i>ARL</i>	16.604	2.370	1.428	1.048	1.003	1.000		
		<i>SDRL</i>	16.601	1.852	0.795	0.218	0.050	0.000		

Table 10. Sensitivity analysis on repetition parameter under pattern 1 when $p = 10$

Control chart	r	(CL_{inner}, CL_{outer})	Criterion	Δ						
				0.1	0.2	0.3	0.5	0.75	1	
<i>RPLR</i>	-	(4.8104, 4.8104)	<i>ARL</i>	71.808	18.923	7.931	3.208	1.776	1.303	
			<i>SDRL</i>	69.230	18.508	7.544	2.698	1.228	0.617	
<i>MDS-RPLR</i>	3	(2.2204, 4.8704)	<i>ARL</i>	67.751	14.509	5.515	1.820	1.135	1.017	
			<i>SDRL</i>	68.836	15.338	5.310	1.444	0.445	0.133	
	4	(2.2239, 4.8832)	<i>ARL</i>	65.510	14.403	5.069	1.725	1.124	1.016	
			<i>SDRL</i>	65.862	14.471	4.938	1.312	0.417	0.131	
	5	(2.2289, 4.9238)	<i>ARL</i>	65.067	13.951	5.064	1.711	1.123	1.015	
			<i>SDRL</i>	65.029	14.184	4.931	1.228	0.416	0.130	
<i>GMDS-RPLR</i>	<i>q = 1</i>	3	(1.7104, 5.0618)	<i>ARL</i>	60.471	11.476	4.365	1.559	1.088	1.006
				<i>SDRL</i>	60.255	11.687	4.091	1.006	0.333	0.080
		4	(1.7139, 5.1266)	<i>ARL</i>	57.509	11.432	4.088	1.554	1.079	1.009
	<i>SDRL</i>			57.421	11.651	3.884	1.026	0.314	0.107	
	5	(1.7189, 5.1672)	<i>ARL</i>	55.819	11.337	4.015	1.505	1.094	1.008	

			<i>SDRL</i>	56.200	12.133	3.816	1.030	0.352	0.095
$q = 2$	3	(1.2978,5.1149)	<i>ARL</i>	60.001	12.261	4.502	1.534	1.048	1.002
			<i>SDRL</i>	60.180	12.124	4.216	0.976	0.226	0.045
	4	(1.3023,5.3500)	<i>ARL</i>	51.906	9.521	3.406	1.340	1.039	1.003
			<i>SDRL</i>	50.403	9.266	3.012	0.717	0.202	0.055
	5	(1.3075,5.4991)	<i>ARL</i>	48.449	8.854	3.072	1.349	1.049	1.004
			<i>SDRL</i>	48.659	8.686	2.645	0.722	0.241	0.063